ACS Catalysis

pubs.acs.org/acscatalysis

Viewpoint

The Case for Enzymatic Competitive Metal Affinity Methods

David J. Reilley, Matthew R. Hennefarth, and Anastassia N. Alexandrova*

Cite This: https://dx.doi.org/10.1021/acscatal.9b04831

Read Online

ACCESS | Metrics & More | Article Recommendations

We often want to know which metal will bind to a protein most readily, which metal or metals actually bind *in vivo*, and which one will be the best at enzymatic catalysis. It is not guaranteed that a single metal could satisfy all of the above for a given natural metalloenzyme. For artificial metalloenzymes (ArMs), we also want to know if the protein can bind to the desired metal and if the metal would then function as a catalyst with the desired activity and selectivity. Hence, being able to compute the metal binding affinities to proteins is desirable in the studies of enzymatic catalysis and enzyme design. Unfortunately, this goal is nontrivial. Efforts toward solving this problem are the focus of this article.

The first step to determine metal affinity is to identify the metal binding site, yet as this is already firmly established for the functional metals of many interesting systems, we will not extensively cover it here. Other papers discuss the development of computational tools to address this particular problem for unstudied, poorly resolved, or less accessible biomolecules. While some of these methods can start from a sequence,[1,2] all eventually require some sort of structure to identify possible binding sites.[3−5] With this constraint, X-ray crystallography remains the most reliable and broadly applicable approach for proteins, even if costly. As with protein folds in general, crystal structures gathered over the last 50 years provide the most likely binding site for a broad range of proteins. As many natural metalloenzymes bind their strongly held metals alongside specifically tailored cofactors, substrates, and scaffolds, the likelihood of other significant binding sites is frequently minimal. However, static structures determined for a predominant metal do not answer all questions of metal affinity and function.

The questions of which metal is used in a natural enzyme and which metal we want to employ in an artificial enzyme are not easily answerable because different forces drive the evolution of enzymes in nature and the priorities of man-made catalysts. Instead of maximizing enzyme activity, biology caps it to maintain the complex equilibria of homeostasis. Biology prioritizes the bioavailability of the starting materials and fold stability but also ensures that enzymes can be readily destroyed when needed. These constraints also apply to the way in which metals are selected for natural metalloenzymes.[6,7] Furthermore, the catalytically relevant metals for many metalloproteins are not truly known. Many enzymes are assumed to be Zn(II) dependent on the basis of the X-ray crystal structures, but this can be an artifact of experimental conditions.[8] Follow-up studies on systems such as histone deacetylase[9,10] carbonic anhydrase,[8] *S*-ribosylhomocysteinase,[11] and peptide deformylase[12] show that sometimes other metals can bind and report significant activity. In some cases, the metal reported by crystallography is not even a particularly significant contributor to the protein's function. Without considering the binding affinity of different metals, *in vitro* and computational studies of metalloproteins could be based on a false or incomplete picture of metal preferences.

A major goal in the design of artificial metalloenzymes is maximal catalytic performance, with less emphasis on stability in their simpler *in vitro* environment of operation. Previous efforts already found that, while proteins provide powerful platforms for new catalysts, the reactions they can perform, and sometimes their catalytic rates, have hard limitations.[13,14] Recently, directed evolution has become an indispensable tool to develop new ArMs or refine existing ones.[15−19] However, directed evolution is constrained by the roles for which a given protein scaffold has evolved.[13,14,20] While there is promiscuity of function in many proteins, some reactions are simply out of reach of conventional methodologies. Metals that are not natively bioavailable can expand the space of accessible reactions. For example, recent efforts show that noble metals can expand the repertoire of porphyrin-dependent enzymes.[21] However, nonphysiological metals must bind sufficiently strongly to their protein scaffolds, whose amino acids did not originally evolve to ligate nonphysiological metals. Thus, the determination of metal affinity is required. Additionally, as we will show shortly, the affinity of the metal to the protein (e.g., the stability gain upon metal binding) and the catalytic activity may follow a nontrivial and nonlinear mutual dependence via the Brønsted−Evans−Polanyi (BEP) relation.

Lastly, metal−protein affinity is of broader interest than biocatalysis. It is relevant to metal transport about the body, particularly the activity of metal chaperones, which unlike many proteins, bind metals in a highly selective manner and in specific environments.[22−25] Chaperones help maintain the distinct metal concentrations in different organ systems, tissues, and even different subcellular organelles within cells.[26] Tracking the metal affinity of these proteins in different contexts is important for metal toxicology. A large number of transition and heavy metals are now bioavailable with their use in modern industries, including industrial catalysis. Some

Received: November 7, 2019
Published: January 17, 2020

https://dx.doi.org/10.1021/acscatal.9b04831
ACS Catal. XXXX, XXX, XXX−XXX

metals, such as Cd(II), Hg(II), As(III), and Pb(II), are highly toxic and lead to nonspecific syndromes.[27,28] The extent of cytotoxicity of other metals, such as Al(III), Ti(IV), and Ga(III), is unclear but demands an investigation as they are introduced into the body both from the environment and for medical purposes.[29−33] Metal binding may even play a role in neurodegenerative diseases, hypothetically facilitating the protein−protein aggregation and fibril formation.[34] Ultimately, it is of high interest to know the metal−protein affinity and have ways to calculate it.

EXISTING METHODS AND THEIR LIMITATIONS

Dedicated computational tools to investigate protein−metal binding, which we will refer to as competitive metal affinity (CMA) methods, are hard to come by. The ideal CMA would incorporate an accurate energy evaluation and significant dynamical sampling to capture configurational entropy in order to fully describe the thermodynamics of metal binding. Clearly, the expense of the accurate energy calculations severely limits the amount of sampling that can be afforded. While there are many methods to study metalloprotein behavior in general, not all are suited to form the basis of a CMA method.

Classical force field based methods can be parametrized to model some metalloenzyme structures but are typically insufficient to obtain thermodynamic values. Force field parameters for metals are based on a point charge supplemented with various harmonic terms and operate on the basis of a fixed metal coordination (e.g., octahedral, tetrahedral) that cannot change significantly as a function of protein dynamics. These potentials can contain bonding and nonbonding interactions but are generally fitted to capture the structure (within limits) rather than energy.[35−38] In this respect, they can be fairly successful for systems containing closed shell metals with ideal geometries (Zn(II), Mg(II), Mn(II), Cd(II)), remaining stable over long molecular dynamics (MD) simulations and providing some thermodynamic data.[39−41] However, even the most successful applications of these methods do not obtain reliable energies for catalytic studies.

Electronic structure calculations are necessary to obtain accurate metal binding energies. One possible approach is to use a small cluster model of the active site and treat it quantum mechanically. However, this approach ignores the entropy of the protein scaffold and the impact of the protein dynamics on the energy and entropy of the active site. The only portion of the entropy in the free energy of the active site that this approach captures is the vibrational entropy, typically calculated within the harmonic approximation and subject to the constraints imposed by the rest of the protein structure. While cluster models are useful for catalytic mechanism mapping[42,43] and as such can play a role in artificial metalloenzyme design,[44−46] these applications rely on the cancellation of errors when protein entropy is ignored equivalently throughout the reaction profile. On the other hand, many metal exchange phenomena are inaccessible to the approach, as enzymes frequently undergo some amount of restructuring when a new metal binds.

A more promising avenue to obtain metal binding free energies based on electronic structure calculations are mixed QM/MM simulations. This class of methods combines a quantum mechanical description of the metal center and its surrounding environment and molecular mechanical modeling of the rest of the protein (Figure 1). Statistical mechanical

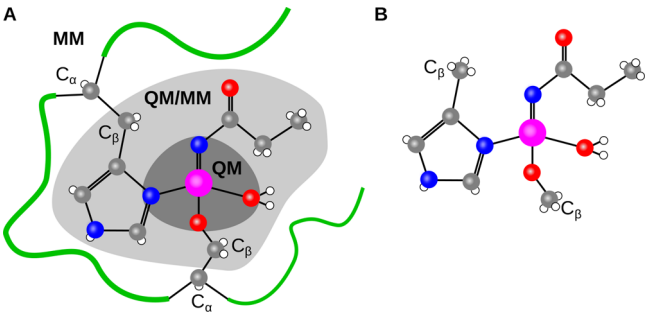

Figure 1. Diagrams demonstrating the active space of (A) QM/MM and (B) small cluster methods. QM/MM models the entire protein with QM for the active site (the dark and light gray regions) and MM for the rest of the protein (the white region). In some forms of QM/MM, such as QM/DMD, there is an overlapping region treated with both QM and MM (in light gray) and MM modeling is only excluded from a small central region (in the case of this diagram, the metal and its first coordination sphere in dark gray). Small cluster methods, in contrast, only model the QM region.

sampling of the protein becomes possible within QM/MM, and there has been intensive research into the development of these methods over the last two decades.[47−49] Sufficient sampling is still a problem, however, for most established QM/MM methods. Our group developed the QM/DMD method,[50] which combines DFT with discrete molecular dynamics (DMD)[51] for enhanced sampling. DMD is based on simplified square-well potentials, ballistic equations of motion, and slight coarse graining, which permit extensive conformational sampling of the full protein. QM/DMD divides the protein into three regions: a QM only region comprising the metal center(s) and ligating atoms, a DMD only region comprising the bulk of the protein, and a region treated with both QM and DMD made up of the rest of the active site (normally composed of 50 to 200 atoms). The overlapping region modeled with both theories allows the geometric and energetic information to pass between QM and DMD calculations. Typically, one step of a QM/DMD simulation involves 10 000 DMD steps followed by a loosely converged DFT geometry optimization. We have used QM/DMD to successfully study many aspects of metalloprotein behavior, including the effect of mutagenesis on structure and function,[50,52,53] metal-dependent catalytic activity,[10,54−56] redox functionality,[50,57] and recently, metal affinity.[10,58] Because of the sampling efficiency and capability of dynamically changing the metal coordination sphere, QM/DMD is suitable for building a CMA technology.

The exact form of the necessary free energy terms is another major complication in the CMA evaluation. One would think that metal affinities could be calculated from some combination of the free energies of the bound metalloprotein, the apoprotein, and the solvated metal ion. This is the approach of standard tools for free energy calculation in QM/MM biomolecular simulations[59,60] including adaptations of thermodynamic integration (TI)[61] and free energy perturbation (FEP).[62] These methods cannot be simply applied to metal binding processes. First, while it would be attractive for metal swapping, there is no accurate way to perform an alchemical transformation directly from one metal to another owing to their distinct electronic structures. Barring this, to obtain metal affinities, these methods would need to model the process of metal binding from solution to protein. However,

https://dx.doi.org/10.1021/acscatal.9b04831
ACS Catal. XXXX, XXX, XXX−XXX

the accuracy of the free energies for these states will depend on the precision of evaluating the entropy change upon binding, which requires complete sampling of the conformational space of the protein both with and without the metal. Such full equilibration is practically impossible.[63] Additionally, evaluations of the free energy of the solvated metal ion require expensive and laborious quantum mechanical treatment, explicit solvent, and sufficient sampling of solvent configurations (on the order of 10^6). As metals are charged, ionic species, obtaining accurate, equilibrated results is more difficult than for the organic molecules to which TI and FEP are applied. Furthermore, this charged nature means that metal ion free energies cannot be directly obtained by the experiment either.[64−66] In what follows, we describe our CMA method that avoids all complications described in this paragraph. We will discuss several diverse applications of the method and its current limitations and propose further directions to improve upon it. To the best of our knowledge, this technique is unprecedented.

THERMODYNAMIC CMA METHOD

Our method calculates the relative metal binding free energy, $\Delta\Delta G$, with respect to one metal chosen as a reference. For many applications, relative free energies are sufficient as at least one metal is already known to bind. The approach combines QM/DMD sampling with a semiempirical thermodynamic cycle that avoids ill-defined terms. First, we employ QM/DMD simulations run to convergence (on the order of 20−100 steps per replicate, which is approximately 10−50 ns of sampling within DMD) of the protein with each considered metal. In the second step, we determine the lowest energy QM region for each metal with optimization of the low-lying structures to tighter convergence and calculate its Gibbs free energy using the harmonic approximation. This approach concentrates on swiftly calculating a limited, but accurate, free energy term for the region about the metal rather than pursuing an arduous and insufficiently accurate full protein free energy. Finally, we use these free energies in a thermodynamic cycle shown in Figure 2. The cycle consists of the metal ions going into the protein from a complex with a chelating agent (typically EDTA, which we exclusively used in all systems described in this article) rather than directly from solution. Hence, instead of using a dubious, calculated value for the free energy of a metal in solution, this cycle uses computationally tractable metal−chelator complexes. The free energies of metal complexation from solution to the chelator are readily available from the experiment. The final step of the cycle cancels the chelator terms through the computed free energies of metal exchange in the protein (from QM/DMD) and in the chelator complex (from *ab initio* or DFT calculations and harmonic vibrational entropies). Closing the thermodynamic cycle yields the $\Delta\Delta G$ of one metal, M_a, binding to the protein relative to the other metal, M_b. This means that, when comparing the results of this method to the experiment, only the trend can be reproduced, not the absolute free energies of metal binding.

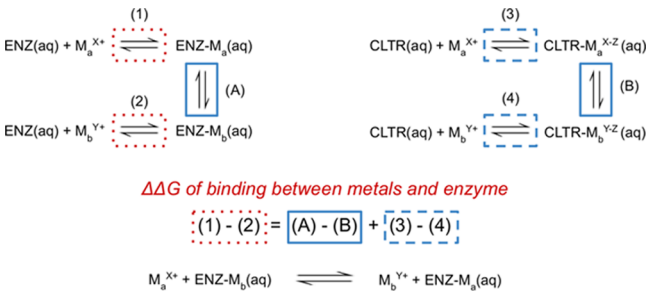

Figure 2. Thermodynamic cycles for the relative free energy of metal binding method. The left cycle of direct enzyme (ENZ) binding is intractable as the structure of the free metal ions in the solution is not defined (dashed red boxes). The right cycle uses experimentally available data for chelator (CLTR) binding to avoid this problem (dashed blue boxes). The sum of this cycle and the easily calculated transition from CLTR to the protein (solid blue boxes) gives the free energy of exchanging metals in the protein by canceling all the CLTR terms.

METHOD BENCHMARK

We have successfully applied the described CMA method to a series of problems of catalytic and biological relevance. To illustrate the method's performance and accuracy, we now describe several diverse examples, each with principally different biological functionality and chemistry. We consider a mononuclear oxidase, a mononuclear metal-dependent hydrolase, and a metal transporter protein.

Acireductone dioxygenase (ARD) can tightly bind different metals and performs different reactions depending on which metal binds. The protein is involved in the methionine salvage pathway and acts on the substrate 1,2-dihydroxy-3-keto-5-(methylthio)pentene, oxidizing it to two possible sets of products.[67,68] ARD bound with Ni(II) catalyzes the formation of methylthiopropinate, while ARD bound with Fe(II) catalyzes the formation of 2-keto-4-methylthiobutyric acid, a precursor of methionine (Figure 3).[69] The bound metal does not change the structure of the protein or the way in which the substrate binds to it, as we showed with QM/DMD. This means that the properties of the metal itself dictate catalytic selectivity. As such, ARD is the subject of many mechanistic studies.[55,70,71] We showed that the mechanistic bifurcation relies on the differences in charge transfer from the metal ligands, through the metal, and to the dioxygen bound to the substrate. Experimental binding studies show that ARD has an appreciable affinity for both Ni(II) and Fe(II).[72,73] The measured activity and metal binding affinities together demonstrate that both ARD reactive pathways are meaningful. The ARD's preference for the metal should then be context dependent. Hence, the relative affinity of ARD to Fe(II) versus Ni(II) in the absence of other environmental factors is of interest.

The application of our CMA method to the catalytic metals in ARD, including Co(II), is illustrated in Table 1. To calculate the binding affinities of Fe(II), Ni(II), and Co(II) to ARD, we started with QM/DMD trajectories from our previous studies.[55] We selected the three lowest energy structures of the QM regions for each metal variant of ARD. We tested all feasible spin states of the metals with further geometry optimizations on these systems, looking for the multiplicity that minimizes the electronic energy. Our calculations showed that the multiplicity of Fe(II) was a singlet or quintet (depending on the structure), Ni(II) was a triplet, and Co(II) was a doublet. For each multiplicity, we then performed frequency calculations and selected the lowest free energy among them. The calculations were done with Turbomole (version 6.6).[74] The pure meta-GGA TPSS DFT functional[75] with the D3 dispersion correction[76] was used. The metal was treated with the triple-ζ basis set def2-TZVPP while all other

https://dx.doi.org/10.1021/acscatal.9b04831
ACS Catal. XXXX, XXX, XXX−XXX

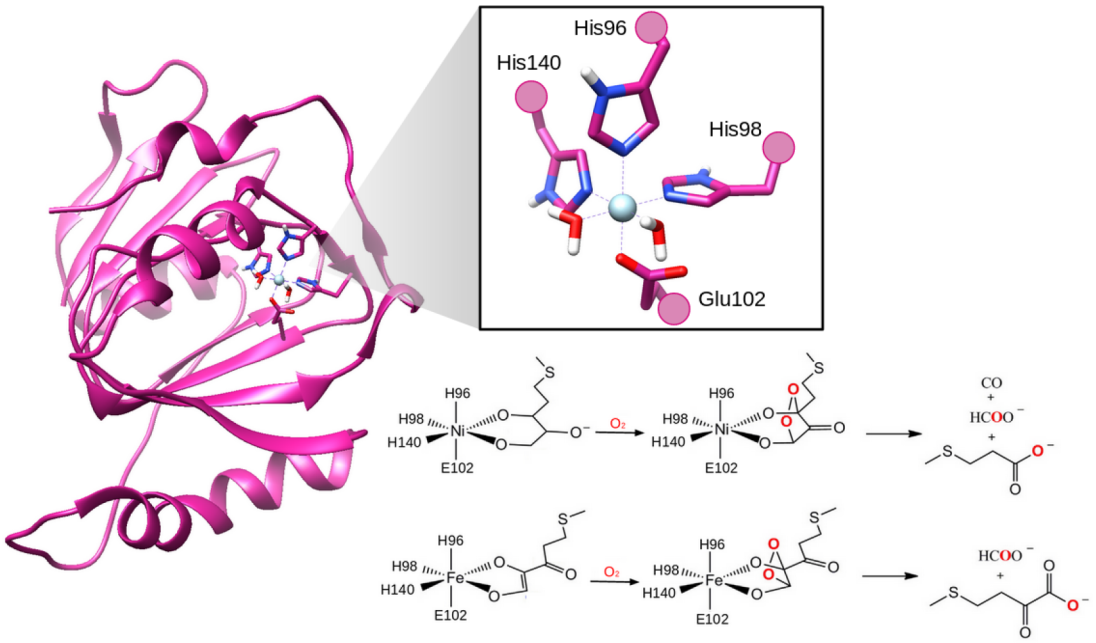

Figure 3. Structure of ARD (PDB ID: 1ZRR) and its active site and the mechanisms of the metal-dependent reactions the protein can perform. The Ni(II) and Fe(II) bound forms of ARD preferentially bind different substrates and therefore perform different reactions.

Table 1. Experimental (Dai and Chai) and Calculated Binding Affinities to ARD[a]

	Fe(II)	Ni(II)	Co(II)
Dai (kcal/mol)	0.0	−1.23	−0.65
Chai (kcal/mol)	0.0	−0.28	N/A
calc. (kcal/mol)	0.0	−3.76	0.38

[a]The energies are relative to Fe(II), which correspondingly has a value of 0 kcal/mol. The experimental values here are based on Boltzmann weighted ratios of molar metal content.

atoms were treated with the double-ζ def2-SVP basis set. The conductor-like Screen Model (COSMO) with a constant dielectric of 20 was used to approximate the screening and solvation effects in the partially buried active site of the protein.[77] We selected this value on the basis of the precedent of our previous, successful simulations of partially exposed active sites (such as the other examples we cover in this article). These settings are consistent with the initial QM/DMD runs. The results correctly capture that the affinity of the

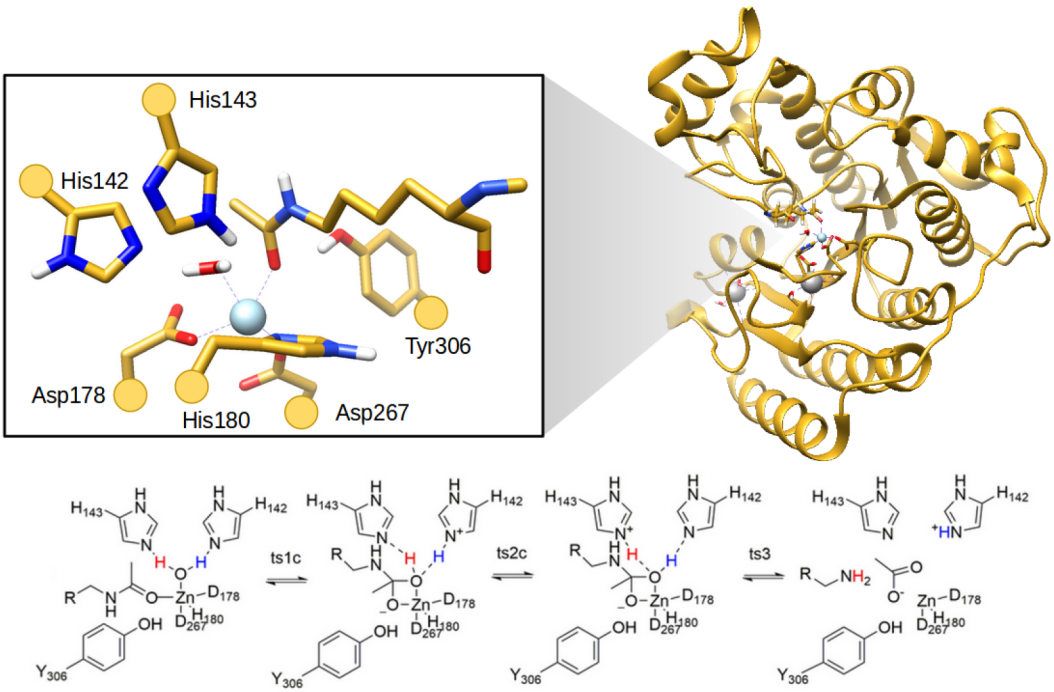

Figure 4. Structure of HDAC8 (PDB ID: 2V5W) and its active site with an example substrate and the most plausible mechanism of the deacetylation reaction it performs.

https://dx.doi.org/10.1021/acscatal.9b04831
ACS Catal. XXXX, XXX, XXX−XXX

Table 2. Experimental k_{cat} and Calculated K_{rel} Values for HDAC8[a]

	Co(II)	Zn(II)	Fe(II)	Ni(II)	Mn(II)	Mg(II)
exp. k_{cat} (s^{-1})	1.2	0.90	0.48	N/A	N/A	N/A
calc. K_{rel}	7.64×10^{-11}	1.27×10^{-11}	1.75×10^{-13}	1.89×10^{-8}	1.37×10^{-17}	1.46×10^{-23}

[a]While the exact values are not comparable, the qualitative order of the two catalytic measures match. Notice that Ni(II) is an exception, with the highest K_{rel} despite its experimental inactivity. Also note that Mg(II) and Mn(II) have K_{rel} values that are many orders of magnitude lower than Co(II), meaning that they are consistent with their inactive experimental result.

protein for Ni(II) is stronger than for Fe(II) and that ARD's affinity for Co(II) is about the same as for Fe(II). The quantitative difference between the computational and experimental values is about 1 to 2 kcal/mol (Table 1). Note that this approaches chemical accuracy (generally accepted as 1 kcal/mol), which is rarely achievable with DFT.[78,79] Given the many approximations needed along the way and despite the cancellation of errors in the relative calculations, the qualitative agreement with the experiment we obtained is still satisfying.

Our next system is a histone deacetylase (HDAC), which is part of a class of enzymes that remove acetyl groups from histone lysines and potentially some nonhistone proteins.[80,81] Alongside histone acetyltransferases, which add acetyl groups, HDACs regulate how tightly histones bind to DNA and therefore gene regulation.[82−84] Overexpression of HDACs is associated with many pathologies, particularly cancer, while inhibition leads to the activation of genes related to growth arrest and tumor cells.[84,85] Consequently, many anticancer drugs are HDAC inhibitors.[86,87] Many of these bind to the transition metal center of their HDAC targets, including FDA approved suberanilohydroxamic acid (Vorinostat)[88] and FK228 (Romidepsin).[89] To reliably develop tighter binding drugs with computational methods, knowledge of which metal or metals bind to HDAC is necessary.

The catalytically relevant metals for histone deacetylases are not well understood. Historically, researchers assumed that HDACs are Zn(II) enzymes on the basis of X-ray structures and kinetic studies.[90,91] While Zn(II) is clearly a catalytically active metal in HDACs, as discussed earlier in this article, the promiscuity of metalloproteins means that crystallographic data does not preclude the relevance of other metals. Indeed, kinetic studies report significant activity for both Co(II) and Fe(II) in HDAC8, with Co(II) showing much higher activity than Zn(II).[9] This variety in metals that HDAC8 can use has important implications in traditional mechanistic studies.

Binding affinities from our method proved necessary to properly identify the catalytically relevant metals besides Zn(II) in HDAC8 and calculate their activities. Our group recently investigated the mechanism of HDAC8 and how it varies with physiologically abundant metals (Zn(II), Fe(II), Co(II), Mn(II), Ni(II), and Mg(II); Figure 4).[10] Pairing a traditional transition state search with QM/DMD simulations, we mapped the mechanism and calculated the activation barrier of the reaction for each metal. However, these results do not capture the experimental catalytic order and suggest that experimentally inactive Mn(II), Ni(II), and Mg(II) are reactive. We theorized that the binding affinities of these metals to HDAC8 contributes to their *in vitro* catalytic activity. We calculated the $\Delta\Delta G$ for each metal and combined this with our computed barriers ($\Delta G^{\ddagger}$) to get a series of K_{rel}:

$$K_{rel} = \exp\left(-\frac{\Delta G^{\ddagger}}{RT}\right)\exp\left(-\frac{\Delta\Delta G_{binding}}{RT}\right)$$

which in contrast to the barriers, match the experimental catalytic order and identify Mn(II) and Mg(II) as inactive (Table 2). The K_{rel} of Ni(II) is the one outlier, with calculations suggesting that it is highly reactive, driven by its predicted high $\Delta\Delta G_{binding}$ rather than $\Delta G^{\ddagger}$. Ultimately, our study of HDAC8 demonstrates the utility of our metal binding $\Delta\Delta G$ method when the catalytic metal or metals of a natural metalloenzyme are not known.

As an aside, we further hypothesize that in some cases the metal binding affinity could be a descriptor of enzymatic catalytic activity. Specifically, by the BEP principle,[92,93] the binding of the rate-determining intermediate to the active site should be neither too strong nor too weak for the maximal catalytic activity to emerge. On the other hand, the stability of the active site itself and the metal ion in it should impact the stability of the intermediate of interest. That is because both the binding energy of the metal to its ligands and the binding energy of the metal to the reaction intermediate depend on the energy and spatial extent of the orbitals of the metal. Therefore, there should be some relationship between the affinity of the protein to the metal and the catalytic activity of the metalloenzyme. We tested this conjecture using the computational data that we generated for the different metal variants of HDAC8, focusing just on the rate-determining, second step of the reaction (as shown in Figure 4). We excluded Mg(II) from the data set, since it is known from the experiment to not bind appreciably to HDAC8. We correlate the $\Delta\Delta G$ of the metal ion binding to the protein to the Boltzmann weighted reaction barriers $e^{-E_a/RT}$ (which are the calculated k_{cat} normalized to remove the pre-exponential factor, which we may assume to be approximately the same for all considered metals). The result is shown in Figure 5. We observe a classic volcano plot (a standard of heterogeneous catalysis analysis for the last 50 years)[94] that all metals obey, even Ni(II), demonstrating peak activity for a binding affinity

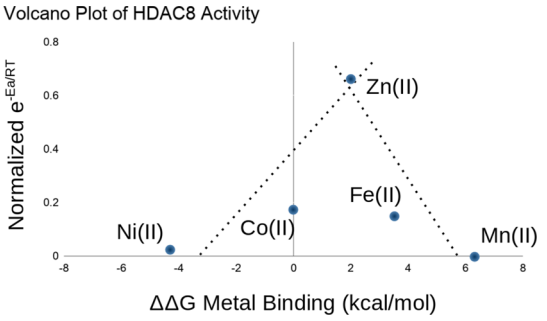

Figure 5. Volcano plot showing the scaling relation of HDAC8 between binding $\Delta\Delta G$ and the reaction rate. We calculated the reaction rates as the Boltzmann weighted ratios between each calculated k_{cat} and the Co(II) reference. The plotted values are normalized to remove the pre-exponential factor, which we may assume to be approximately the same for all considered metals. Notice how even Ni(II) is consistent with this trend.

https://dx.doi.org/10.1021/acscatal.9b04831
ACS Catal. XXXX, XXX, XXX−XXX

around that of Zn(II). While we cannot assume that all metalloenzymes obey this sort of scaling relation, this demonstrates the utility of CMAs for yet another catalytic application.

Human serum transferrin (hTF) is an example of how CMAs could be used in a different context. This protein is not catalytic but is interesting for the purpose of this article because it can uptake and also release metals through pH-dependent protein conformations with potentially profound implications in metal toxicology. The protein natively moves iron into cells by receptor-mediated endocytosis. Since it can cross the blood−brain barrier and its receptor is overexpressed in some cancer cells, hTF brings its cargo into particularly sensitive parts of the body.[95,96] Alarmingly, *in vitro* binding studies show that hTF can bind other metals besides Fe(III),[97−99] including the potentially cytotoxic Ti(IV), Al(III), and Ga(III).[29,33] The promiscuity of hTF is of medical concern as these toxic metals are increasingly bioavailable with their use in modern industries, including in therapeutic drugs.[32,33,100,101] Previous studies provide some structural details on how hTF transports metals, but none access its full *in vivo* activity. Two domains comprise the protein, each of which binds a single metal atom between two, highly similar subdomain lobes. Crystal structures and X-ray absorption fine structure spectroscopy studies of the N-terminal domain suggest that the lobes hinge open in the endosome environment (Figure 6).[102] Such a conformational change

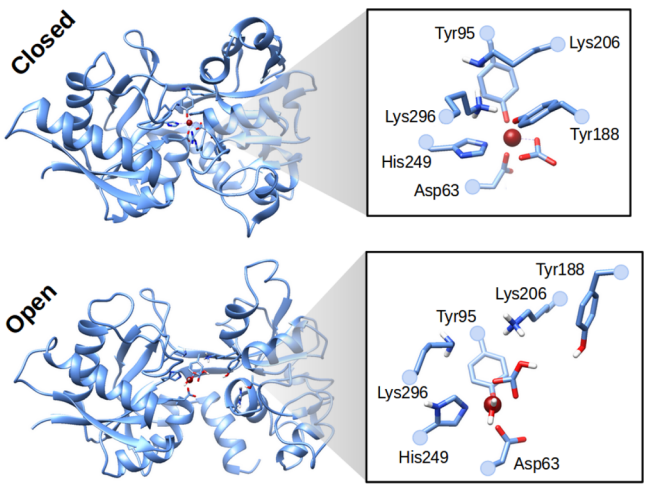

Figure 6. Structure of hTF and its active site in the closed and open forms of the protein. The closed form is associated with the pH of the blood serum, while the open form is associated with the low pH conditions of the endosome. The closed structure was obtained by X-ray crystallography (PDB ID: 3V83), while the open structure was obtained from computational studies.[58]

encourages metal release. Previous classical MD simulations could access the protein opening[103,104] but not the thermodynamic data about the metal release.

We used our CMA method to get the first insight into the toxic metal transport abilities of hTF *in vivo* conformational states. We calculated metal binding affinities relative to physiological Fe(III) for Ti(IV), Co(III), Ga(III), Cr(III), Fe(II), and Zn(II) in both uptake and release implicated forms of hTF (Figure 7).[58] The order of the binding affinities in the uptake form of the protein is qualitatively consistent with the experiment. Accordingly, as Ti(IV), Co(III), Ga(III), and Cr(III) demonstrate $\Delta\Delta G$ that are negative or about 0 in this form, our results show that hTF can uptake these given metals competitively with Fe(III). In contrast, the results for the release states vary for these metals, with Co(III) and Cr(III) reporting consistently large $\Delta\Delta G$ but Ti(IV) and Ga(III) reporting small or negative $\Delta\Delta G$ in one form. This suggests that hTF releases Co(III) and Cr(III) much more readily than Fe(III) but releases Ti(IV) and Ga(III) about as readily as Fe(III). Since Ti(IV) and Ga(III) strongly bind to both the closed and open states, these cytotoxic metals may sequester some of the protein. Further, our study identified the protein residues that are most likely to be responsible for opening and closing at changing pH values as well as a collection of geometric and electronic factors that are responsible for the different affinities of hTF to the studied metals.

LIMITATIONS AND OUTLOOK

Further research into CMA methods is important, especially as our method is not without limitations. Its reliance on chelating agents introduces other problems besides limiting calculations to referential $\Delta\Delta G$. The best way to calculate the thermodynamic terms involving the chelating agent is unclear. Experimental stability constants for EDTA and many related chelating agents are fortunately available for most metals in their common oxidation states.[105] Unfortunately, the corresponding structures of these metal complexes are not fully known, and they are necessary to accurately calculate the free energy associated with the transition from the chelator complex to the protein. In the studies we discuss above, we assume full chelation of each metal with no other ligands in the complexes. This makes most metals conform to an octahedral geometry. This is likely fine for large transition metals but breaks down for small and low charge metals such as Li(I) and Mg(II). Indeed, crystallographic studies of Mg-EDTA binding show that a water molecule is also a ligand in the complex.[106] One way to mitigate these problems would be a benchmark study of a wide range of chelators on a system that has been experimentally well characterized for many metals. Calculating the set of $\Delta\Delta G$ for each chelator without varying any other parameters would reveal which chelator can be used most accurately for each metal.

Our method is also limited to proteins that undergo only minor conformational changes upon the binding of different metals. The first concern here is that the QM regions must share the same atoms besides the metal center to satisfy the thermodynamic cycle. Metals that bind entirely different sites on a protein are consequentially inaccessible to our current method. A second concern largely involves computational scaling, as a significant rearrangement (like refolding) upon metal binding requires even more expensive structural sampling in order to accurately assess the entropy component of $\Delta\Delta G$. While this is a general problem with protein and metalloprotein simulations, enhanced sampling for the specific purpose of metal binding affinities would be impactful. Solutions to both of these concerns would render many systems more accessible, particularly metal chaperones as these proteins can adopt different folds for different metals.[24]

Our current CMA is also limited in accuracy and chemical scope by its use of DFT. Traditionally, DFT struggles with multireference systems, where one Slater determinant or configuration state function is insufficient, especially metal clusters. Certain post-Hartree−Fock wave function methods can appropriately treat these cases and are particularly

https://dx.doi.org/10.1021/acscatal.9b04831
ACS Catal. XXXX, XXX, XXX−XXX

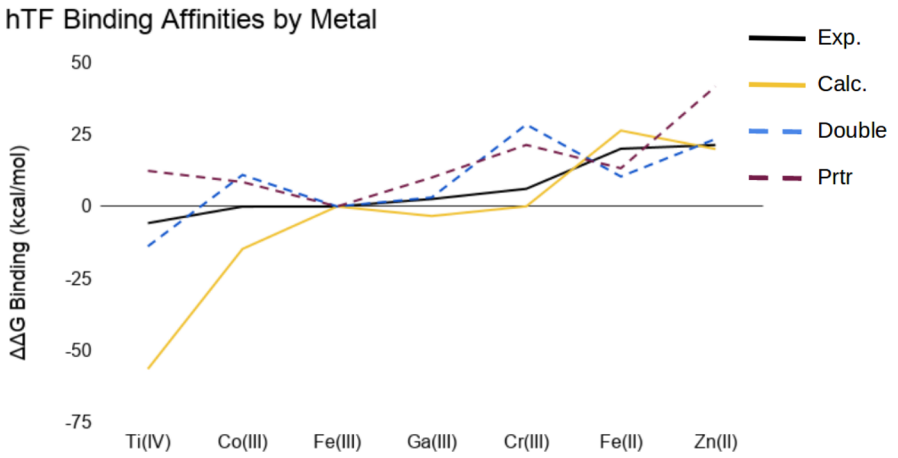

Figure 7. Metal binding affinities to hTF from the experiment (solid black line) and from our method. All affinities are relative to Fe(III), which correspondingly has a value of 0 kcal/mol for all lines. The experimental values are based on Boltzmann weighted ratios of binding constants. The solid yellow line shows the values from the uptake form of the protein. Notice that it matches the shape and order of the experimental line. Furthermore, note that Ti(IV), Co(III), Ga(III), and Cr(III) all have values that are negative or around 0 for this line. The dashed light blue and dark purple lines are the values from the release forms of the protein (called "Double" and "Prtr"). The difference between the two forms is minor but significant; the structure represented with the light blue line contains an additional water molecule in its active site. Notice that, for at least one of the dashed lines, both Ti(IV) and Ga(III) bind about the same or better than Fe(III).

important for accurate energies. There is already much discussion on the use of these tools in heterogeneous catalysis.[107] As multireference post-Hartree−Fock methods tend to be computationally intensive, the multiconfiguration pair-density functional theory that blends wave function methods with DFT is promising for CMA applications because of their affordability.[108] Future CMAs could use such methods specifically for the free energy calculations on the QM region to obtain more accurate energies without increasing computational cost too drastically.

Further advancements in CMA methods would greatly propel the understanding of natural metalloenzymes and the design of new ArMs. Such techniques could determine the catalytically relevant metals in natural metalloenzymes, which cannot be taken for granted from crystal structures. CMA calculations would be indispensable in the effort to better understand metal transport pathways throughout the body, especially with regards to metal toxicology. In the design of ArMs, replacing the bound metal in an existing metalloprotein scaffold can introduce new functions, often inaccessible to current design methodologies like directed evolution. Placing a metal into a specifically designed artificial scaffold is also an attractive opportunity for ArMs catalysis. For all such design tasks, it is critical to assess the metal affinity and its ability to outperform other metals that might be present in the synthesis conditions. New tools such as CMAs will expand the catalytic space of metalloenzymes.

AUTHOR INFORMATION

Corresponding Author

Anastassia N. Alexandrova − *Department of Chemistry and Biochemistry and California NanoSystems Institute, University of California, Los Angeles, Los Angeles, California 90095-1569, United States;* orcid.org/0000-0002-3003-1911; Phone: +1 310 8253769; Email: ana@chem.ucla.edu

Authors

David J. Reilley − *Department of Chemistry and Biochemistry, University of California, Los Angeles, Los Angeles, California 90095-1569, United States*

Matthew R. Hennefarth − *Department of Chemistry and Biochemistry, University of California, Los Angeles, Los Angeles, California 90095-1569, United States*

Complete contact information is available at: https://pubs.acs.org/10.1021/acscatal.9b04831

Notes

The authors declare no competing financial interest.

ACKNOWLEDGMENTS

We thank the Institute for Digital Research and Education at UCLA and the Extreme Science and Engineering Discovery Environment for supercomputer time. The support for this work over the years came from the NSF-CAREER Award CHE-1351968, NSFCHE-1903808, and NIGMS 1R01GM134047.

REFERENCES

(1) Levy, R.; Edelman, M.; Sobolev, V. Prediction of 3D Metal Binding Sites From Translated Gene Sequences Based on Remote-Homology Templates. *Proteins: Struct., Funct., Genet.* **2009**, *76*, 365−374.

(2) Passerini, A.; Lippi, M.; Frasconi, P. MetalDetector v2.0: Predicting the Geometry of Metal Binding Sites From Protein Sequence. *Nucleic Acids Res.* **2011**, *39*, W288−W292.

(3) Sodhi, J. S.; Bryson, K.; McGuffin, L. J.; Ward, J. J.; Wernisch, L.; Jones, D. T. Predicting Metal-Binding Site Residues in Low-Resolution Structural Models. *J. Mol. Biol.* **2004**, *342*, 307−320.

(4) Zheng, H.; Chordia, M. D.; Cooper, D. R.; Chruszcz, M.; Müller, P.; Sheldrick, G. M.; Minor, W. Validation of Metal-Binding Sites in Macromolecular Structures With the CheckMyMetal Web Server. *Nat. Protoc.* **2014**, *9*, 156.

(5) Giambasu, G. M.; Case, D. A.; York, D. M. Predicting Site-Binding Modes of Ions and Water to Nucleic Acids Using Molecular Solvation Theory. *J. Am. Chem. Soc.* **2019**, *141*, 2435−2445.

(6) Kepp, K. P. Heme: From Quantum Spin Crossover to Oxygen Manager of Life. *Coord. Chem. Rev.* **2017**, *344*, 363−374.

(7) Valdez, C. E.; Smith, Q. A.; Nechay, M. R.; Alexandrova, A. N. Mysteries of Metals in Metalloenzymes. *Acc. Chem. Res.* **2014**, *47*, 3110−3117.

https://dx.doi.org/10.1021/acscatal.9b04831
ACS Catal. XXXX, XXX, XXX−XXX

(8) Tripp, B. C.; Bell, C. B.; Cruz, F.; Krebs, C.; Ferry, J. G. A Role for Iron in an Ancient Carbonic Anhydrase. *J. Biol. Chem.* **2004**, *279*, 6683−6687.
(9) Gantt, S. L.; Gattis, S. G.; Fierke, C. A. Catalytic Activity and Inhibition of Human Histone Deacetylase 8 is Dependent on the Identity of the Active Site Metal Ion. *Biochemistry* **2006**, *45*, 6170−6178.
(10) Nechay, M. R.; Gallup, N. M.; Morgenstern, A.; Smith, Q. A.; Eberhart, M. E.; Alexandrova, A. N. Histone Deacetylase 8: Characterization of Physiological Divalent Metal Catalysis. *J. Phys. Chem. B* **2016**, *120*, 5884−5895.
(11) Zhu, J.; Dizin, E.; Hu, X.; Wavreille, A.-S.; Park, J.; Pei, D. S-Ribosylhomocysteinase (LuxS) is a Mononuclear Iron Protein. *Biochemistry* **2003**, *42*, 4717−4726.
(12) Rajagopalan, P. R.; Yu, X. C.; Pei, D. Peptide Deformylase: a New Type of Mononuclear Iron Protein. *J. Am. Chem. Soc.* **1997**, *119*, 12418−12419.
(13) Renata, H.; Wang, Z. J.; Arnold, F. H. Expanding the Enzyme Universe: Accessing Non-Natural Reactions by Mechanism-Guided Directed Evolution. *Angew. Chem., Int. Ed.* **2015**, *54*, 3351−3367.
(14) Hyster, T. K.; Ward, T. R. Genetic Optimization of Metalloenzymes: Enhancing Enzymes for Non-Natural Reactions. *Angew. Chem., Int. Ed.* **2016**, *55*, 7344−7357.
(15) Fasan, R.; Meharenna, Y. T.; Snow, C. D.; Poulos, T. L.; Arnold, F. H. Evolutionary History of a Specialized P450 Propane Monooxygenase. *J. Mol. Biol.* **2008**, *383*, 1069−1080.
(16) Lewis, J. C.; Bastian, S.; Bennett, C. S.; Fu, Y.; Mitsuda, Y.; Chen, M. M.; Greenberg, W. A.; Wong, C.-H.; Arnold, F. H. Chemoenzymatic Elaboration of Monosaccharides Using Engineered Cytochrome P450BM3 Demethylases. *Proc. Natl. Acad. Sci. U. S. A.* **2009**, *106*, 16550−16555.
(17) Rentmeister, A.; Brown, T. R.; Snow, C. D.; Carbone, M. N.; Arnold, F. H. Engineered bacterial mimics of human drug metabolizing enzyme CYP2C9. *ChemCatChem* **2011**, *3*, 1065−1071.
(18) Yu, F.; Cangelosi, V. M.; Zastrow, M. L.; Tegoni, M.; Plegaria, J. S.; Tebo, A. G.; Mocny, C. S.; Ruckthong, L.; Qayyum, H.; Pecoraro, V. L. Protein Design: Toward Functional Metalloenzymes. *Chem. Rev.* **2014**, *114*, 3495−3578.
(19) Reetz, M. T. Directed Evolution of Artificial Metalloenzymes: A Universal Means to Tune the Selectivity of Transition Metal Catalysts? *Acc. Chem. Res.* **2019**, *52*, 336−344.
(20) Prier, C. K.; Arnold, F. H. Chemomimetic Biocatalysis: Exploiting the Synthetic Potential of Cofactor-Dependent Enzymes to Create New Catalysts. *J. Am. Chem. Soc.* **2015**, *137*, 13992−14006.
(21) Natoli, S. N.; Hartwig, J. F. Noble- Metal Substitution in Hemoproteins: An Emerging Strategy for Abiological Catalysis. *Acc. Chem. Res.* **2019**, *52*, 326−335.
(22) Finney, L. A.; O'Halloran, T. V. Transition Metal Speciation in the Cell: Insights from the Chemistry of Metal Ion Receptors. *Science* **2003**, *300*, 931−936.
(23) Tottey, S.; Harvie, D. R.; Robinson, N. J. Understanding How Cells Allocate Metals Using Metal Sensors and Metallochaperones. *Acc. Chem. Res.* **2005**, *38*, 775−783.
(24) Tottey, S.; Waldron, K. J.; Firbank, S. J.; Reale, B.; Bessant, C.; Sato, K.; Cheek, T. R.; Gray, J.; Banfield, M. J.; Dennison, C.; Robinson, N. J. Protein-Folding Location Can Regulate Manganese-Binding Versus Copper-or Zinc-Binding. *Nature* **2008**, *455*, 1138.
(25) Foster, A. W.; Osman, D.; Robinson, N. J. Metal Preferences and Metallation. *J. Biol. Chem.* **2014**, *289*, 28095−28103.
(26) Xiao, Z.; Wedd, A. G. The Challenges of Determining Metal−Protein Affinities. *Nat. Prod. Rep.* **2010**, *27*, 768−789.
(27) Pieczenik, S. R.; Neustadt, J. Mitochondrial Dysfunction and Molecular Pathways of Disease. *Exp. Mol. Pathol.* **2007**, *83*, 84−92.
(28) Ibrahim, D.; Froberg, B.; Wolf, A.; Rusyniak, D. E. Heavy Metal poisoning: clinical Presentations and Pathophysiology. *Clin. Lab. Med.* **2006**, *26*, 67−97.
(29) Exley, C.; Burgess, E.; Day, J. P.; Jeffery, E. H.; Yokel, R. A. Aluminum Toxicokinetics. *J. Toxicol. Environ. Health* **1996**, *48*, 569−584.
(30) Tinoco, A. D.; Thomas, H. R.; Incarvito, C. D.; Saghatelian, A.; Valentine, A. M. Cytotoxicity of a Ti (IV) Compound is Independent of Serum Proteins. *Proc. Natl. Acad. Sci. U. S. A.* **2012**, *109*, 5016−5021.
(31) Guo, M.; Sun, H.; McArdle, H. J.; Gambling, L.; Sadler, P. J. TiIV Uptake and Release by Human Serum Transferrin and Recognition of TiIV-Transferrin by Cancer Cells: Understanding the Mechanism of Action of the Anticancer Drug Titanocene Dichloride. *Biochemistry* **2000**, *39*, 10023−10033.
(32) Jakupec, M. A.; Keppler, B. K. Gallium in Cancer Treatment. *Curr. Top. Med. Chem.* **2004**, *4*, 1575−1583.
(33) Exley, C. Human Exposure to Aluminium. *Environ. Sci.: Processes Impacts* **2013**, *15*, 1807−1816.
(34) Gaggelli, E.; Kozlowski, H.; Valensin, D.; Valensin, G. Copper Homeostasis and Neurodegenerative Disorders (Alzheimer's, Prion, and Parkinson's diseases and Amyotrophic Lateral Sclerosis). *Chem. Rev.* **2006**, *106*, 1995−2044.
(35) Hoops, S. C.; Anderson, K. W.; Merz, K. M., Jr Force Field Design for Metalloproteins. *J. Am. Chem. Soc.* **1991**, *113*, 8262−8270.
(36) Dal Peraro, M.; Spiegel, K.; Lamoureux, G.; De Vivo, M.; DeGrado, W. F.; Klein, M. L. Modeling the Charge Distribution at Metal Sites in Proteins for Molecular Dynamics Simulations. *J. Struct. Biol.* **2007**, *157*, 444−453.
(37) Neves, R. P.; Sousa, S. F.; Fernandes, P. A.; Ramos, M. J. Parameters for molecular dynamics simulations of manganese-containing metalloproteins. *J. Chem. Theory Comput.* **2013**, *9*, 2718−2732.
(38) Cho, A. E.; Goddard, W. A., III *Metalloproteins: theory, calculations, and experiments*; CRC Press: Boca Raton, FL, 2015.
(39) Dal Peraro, M.; Vila, A. J.; Carloni, P.; Klein, M. L. Role of Zinc Content on the Catalytic Efficiency of B1Metallo β-lactamases. *J. Am. Chem. Soc.* **2007**, *129*, 2808−2816.
(40) Zhang, J.; Yang, W.; Piquemal, J.-P.; Ren, P. Modeling Structural Coordination and Ligand Binding in Zinc Proteins with a Polarizable Potential. *J. Chem. Theory Comput.* **2012**, *8*, 1314−1324.
(41) Panteva, M. T.; Giambasu, G. M.; York, D. M. Force Field for Mg2+, Mn2+, Zn2+, and Cd2+ Ions that Have Balanced Interactions with Nucleic Acids. *J. Phys. Chem. B* **2015**, *119*, 15460−15470.
(42) Rydberg, P.; Sigfridsson, E.; Ryde, U. On the Role of the Axial Ligand in Heme Proteins: a Theoretical Study. *JBIC, J. Biol. Inorg. Chem.* **2004**, *9*, 203−223.
(43) Tantillo, D. J. How an Enzyme Might Accelerate an Intramolecular Diels-Alder Reaction: Theozymes for the Formation of Salvileucalin B. *Org. Lett.* **2010**, *12*, 1164−1167.
(44) Kries, H.; Blomberg, R.; Hilvert, D. De Novo Enzymes by Computational Design. *Curr. Opin. Chem. Biol.* **2013**, *17*, 221−228.
(45) Kiss, G.; Çelebi-Ölçüm, N.; Moretti, R.; Baker, D.; Houk, K. Computational Enzyme Design. *Angew. Chem., Int. Ed.* **2013**, *52*, 5700−5725.
(46) Vaissier Welborn, V.; Head-Gordon, T. Computational Design of Synthetic Enzymes. *Chem. Rev.* **2019**, *119*, 6613−6630.
(47) Blomberg, M. R.; Borowski, T.; Himo, F.; Liao, R.-Z.; Siegbahn, P. E. Quantum Chemical Studies of Mechanisms for Metalloenzymes. *Chem. Rev.* **2014**, *114*, 3601−3658.
(48) Ryde, U. In *Methods in Enzymology*; Elsevier, 2016; Vol. *577*; pp 119−158.
(49) Ahmadi, S.; Barrios Herrera, L.; Chehelamirani, M.; Hostaš, J.; Jalife, S.; Salahub, D. R. Multiscale Modeling of Enzymes: QM-Cluster, QM/MM, and QM/MM/MD: A Tutorial Review. *Int. J. Quantum Chem.* **2018**, *118*, e25558.
(50) Sparta, M.; Shirvanyants, D.; Ding, F.; Dokholyan, N. V.; Alexandrova, A. N. Hybrid Dynamics Simulation Engine for Metalloproteins. *Biophys. J.* **2012**, *103*, 767−776.
(51) Ding, F.; Tsao, D.; Nie, H.; Dokholyan, N. V. Ab Initio Folding of Proteins with All-Atom Discrete Molecular Dynamics. *Structure* **2008**, *16*, 1010−1018.
(52) Valdez, C. E.; Morgenstern, A.; Eberhart, M. E.; Alexandrova, A. N. Predictive Methods for Computational Metalloenzyme

https://dx.doi.org/10.1021/acscatal.9b04831
ACS Catal. XXXX, XXX, XXX−XXX

Redesign − A Test Case with Carboxypeptidase A. *Phys. Chem. Chem. Phys.* **2016**, *18*, 31744−31756.
(53) Reilley, D. J.; Popov, K.; Dokholyan, N. V.; Alexandrova, A. N. Uncovered Dynamic Coupling Resolves the Ambiguous Mechanism of Phenylalanine Hydroxylase Oxygen Binding. *J. Phys. Chem. B* **2019**, *123*, 4534−4539.
(54) Valdez, C. E.; Alexandrova, A. N. Why Urease is a Di-Nickel Enzyme Whereas the CcrA β-lactamase is a Di-Zinc Enzyme. *J. Phys. Chem. B* **2012**, *116*, 10649−10656.
(55) Sparta, M.; Valdez, C. E.; Alexandrova, A. N. Metal-Dependent Activity of Fe and Ni Acireductone Dioxygenases: How Two Electrons Reroute the Catalytic Pathway. *J. Mol. Biol.* **2013**, *425*, 3007−3018.
(56) Valdez, C. E.; Gallup, N. M.; Alexandrova, A. N. Co^{2+} Acireductone Dioxygenase: Fe^{2+} Mechanism, Ni^{2+} Mechanism, or Something Else? *Chem. Phys. Lett.* **2014**, *604*, 77−82.
(57) Nedd, S.; Redler, R. L.; Proctor, E. A.; Dokholyan, N. V.; Alexandrova, A. N. Cu, Zn-Superoxide Dismutase Without Zn is Folded but Catalytically Inactive. *J. Mol. Biol.* **2014**, *426*, 4112−4124.
(58) Reilley, D. J.; Fuller, J. T., III; Nechay, M. R.; Victor, M.; Li, W.; Ruberry, J. D.; Mujika, J. I.; Lopez, X.; Alexandrova, A. N. Toxic and Physiological Metal Uptake and Release by Human Serum Transferrin: Insight from QM/MM Dynamics Simulations. **2019**, submitted for publication.
(59) Kästner, J.; Senn, H. M.; Thiel, S.; Otte, N.; Thiel, W. QM/MM Free-Energy Perturbation Compared to Thermodynamic Integration and Umbrella Sampling: Application to an Enzymatic Reaction. *J. Chem. Theory Comput.* **2006**, *2*, 452−461.
(60) Giese, T. J.; York, D. M. Development of a Robust Indirect Approach for MM QM Free Energy Calculations That Combines Force-Matched Reference Potential and Bennett's Acceptance Ratio Methods. *J. Chem. Theory Comput.* **2019**, *15*, 5543−5562.
(61) Kirkwood, J. G. Statistical Mechanics of Fluid Mixtures. *J. Chem. Phys.* **1935**, *3*, 300−313.
(62) Zwanzig, R. W. High-Temperature Equation of State by a Perturbation Method. I. Nonpolar Gases. *J. Chem. Phys.* **1954**, *22*, 1420−1426.
(63) Genheden, S.; Ryde, U. Will Molecular Dynamics Simulations of Proteins Ever Reach Equilibrium? *Phys. Chem. Chem. Phys.* **2012**, *14*, 8662−8677.
(64) Guggenheim, E. The Conceptions of Electrical Potential Difference Between Two Phases and the Individual Activities of Ions. *J. Phys. Chem.* **1929**, *33*, 842−849.
(65) Klotz, I. M.; Rosenberg, R. M. *Chemical Thermodynamics*; Wiley: New York, NY, 1994.
(66) Kelly, C. P.; Cramer, C. J.; Truhlar, D. G. Aqueous Solvation Free Energies of Ions and Ion- water clusters Based on an Accurate Value for the Absolute Aqueous Solvation Free Energy of the Proton. *J. Phys. Chem. B* **2006**, *110*, 16066−16081.
(67) Myers, R. W.; Wray, J.; Fish, S.; Abeles, R. Purification and Characterization of an Enzyme Involved in Oxidative Carbon-Carbon Bond Cleavage Reactions in the Methionine Salvage Pathway of Klebsiella pneumoniae. *J. Biol. Chem.* **1993**, *268*, 24785−24791.
(68) Oram, S. W.; Ai, J.; Pagani, G. M.; Hitchens, M. R.; Stern, J. A.; Eggener, S.; Pins, M.; Xiao, W.; Cai, X.; Haleem, R.; Jiang, F.; Pochapsky, T. C.; Hedstrom, L.; Wang, Z. Expression and Function of the Human Androgen-Responsive Gene ADI1 in Prostate Cancer. *Neoplasia* **2007**, *9*, 643.
(69) Dai, Y.; Wensink, P. C.; Abeles, R. H. One Protein, Two Enzymes. *J. Biol. Chem.* **1999**, *274*, 1193−1195.
(70) Wray, J. W.; Abeles, R. H. The Methionine Salvage Pathway in Klebsiella pneumoniae and Rat Liver Identification and Characterization of Two Novel Dioxygenases. *J. Biol. Chem.* **1995**, *270*, 3147−3153.
(71) Borowski, T.; Bassan, A.; Siegbahn, P. E. DFT Study of the Uncatalyzed Dioxygenation of Acireductone. *J. Mol. Struct.: THEOCHEM* **2006**, *772*, 89−92.
(72) Dai, Y.; Pochapsky, T. C.; Abeles, R. H. Mechanistic Studies of Two Dioxygenases in the Methionine Salvage Pathway of Klebsiella pneumoniae. *Biochemistry* **2001**, *40*, 6379−6387.
(73) Chai, S. C.; Ju, T.; Dang, M.; Goldsmith, R. B.; Maroney, M. J.; Pochapsky, T. C. Characterization of Metal Binding in the Active Sites of Acireductone Dioxygenase Isoforms from Klebsiella ATCC 8724. *Biochemistry* **2008**, *47*, 2428−2438.
(74) *Turbomole*, V. 6.6; Turbomole Gmbh: Karlsruhe, Germany, 2014.
(75) Staroverov, V. N.; Scuseria, G. E.; Tao, J.; Perdew, J. P. Comparative Assessment of a New Nonempirical Density Functional: Molecules and Hydrogen-Bonded Complexes. *J. Chem. Phys.* **2003**, *119*, 12129−12137.
(76) Grimme, S.; Antony, J.; Ehrlich, S.; Krieg, H. A Consistent and Accurate Ab Initio Parametrization of Density Functional Dispersion Correction (DFT-D) for the 94 Elements H-Pu. *J. Chem. Phys.* **2010**, *132*, 154104.
(77) Klamt, A. Conductor-Like Screening Model for Real Solvents: a New Approach to the Quantitative Calculation of Solvation Phenomena. *J. Phys. Chem.* **1995**, *99*, 2224−2235.
(78) Cramer, C. J.; Truhlar, D. G. Density Functional Theory for Transition Metals and Transition Metal Chemistry. *Phys. Chem. Chem. Phys.* **2009**, *11*, 10757−10816.
(79) Mardirossian, N.; Head-Gordon, M. Thirty Years of Density Functional Theory in Computational Chemistry: an Overview and Extensive Assessment of 200 Density Functionals. *Mol. Phys.* **2017**, *115*, 2315−2372.
(80) Kouzarides, T. Acetylation: a Regulatory Modification to Rival Phosphorylation? *EMBO J.* **2000**, *19*, 1176−1179.
(81) Choudhary, C.; Kumar, C.; Gnad, F.; Nielsen, M. L.; Rehman, M.; Walther, T. C.; Olsen, J. V.; Mann, M. Lysine Acetylation Targets Protein Complexes and Co-Regulates Major Cellular Functions. *Science* **2009**, *325*, 834−840.
(82) Phillips, D. The Presence of Acetyl Groups in Histones. *Biochem. J.* **1963**, *87*, 258.
(83) Allfrey, V.; Faulkner, R.; Mirsky, A. Acetylation and Methylation of Histones and Their Possible Role in he Regulation of RNA Synthesis. *Proc. Natl. Acad. Sci. U. S. A.* **1964**, *51*, 786−794.
(84) Gallinari, P.; Di Marco, S.; Jones, P.; Pallaoro, M.; Steinkühler, C. HDACs, Histone Deacetylation and Gene Transcription: From Molecular Biology to Cancer Therapeutics. *Cell Res.* **2007**, *17*, 195.
(85) Haberland, M.; Montgomery, R. L.; Olson, E. N. The Many Roles of Histone Deacetylases in Development and Physiology: Implications for Disease and Therapy. *Nat. Rev. Genet.* **2009**, *10*, 32.
(86) Marks, P. A.; Breslow, R. Dimethyl Sulfoxide to Vorinostat: Development of This Histone Deacetylase Inhibitor as an Anticancer Drug. *Nat. Biotechnol.* **2007**, *25*, 84.
(87) West, A. C.; Johnstone, R. W. New and Emerging HDAC Inhibitors for Cancer Treatment. *J. Clin. Invest.* **2014**, *124*, 30−39.
(88) Lobera, M.; Madauss, K. P.; Pohlhaus, D. T.; Wright, Q. G.; Trocha, M.; Schmidt, D. R.; Baloglu, E.; Trump, R. P.; Head, M. S.; Hofmann, G. A.; Murray-Thompson, M.; Schwartz, B.; Chakravorty, S.; Wu, Z.; Mander, P. K.; Kruidenier, L.; Reid, R. A.; Burkhart, W.; Turunen, B. J.; Rong, J. X.; Wagner, C.; Moyer, M. B.; Wells, C.; Hong, X.; Moore, J. T.; Williams, J. D.; Soler, D.; Ghosh, S.; Nolan, M. A. Selective Class IIa Histone Deacetylase Inhibition Via a Nonchelating Zinc-Binding Group. *Nat. Chem. Biol.* **2013**, *9*, 319.
(89) Furumai, R.; Matsuyama, A.; Kobashi, N.; Lee, K.-H.; Nishiyama, M.; Nakajima, H.; Tanaka, A.; Komatsu, Y.; Nishino, N.; Yoshida, M.; Horinouchi, S. FK228 (Depsipeptide) as a Natural Prodrug That Inhibits Class I Histone Deacetylases. *Cancer Res.* **2002**, *62*, 4916−4921.
(90) Finnin, M. S.; Donigian, J. R.; Cohen, A.; Richon, V. M.; Rifkind, R. A.; Marks, P. A.; Breslow, R.; Pavletich, N. P. Structures of a Histone Deacetylase Homologue Bound to the TSA and SAHA Inhibitors. *Nature* **1999**, *401*, 188.
(91) Drummond, D. C.; Noble, C. O.; Kirpotin, D. B.; Guo, Z.; Scott, G. K.; Benz, C. C. Clinical Development of Histone

https://dx.doi.org/10.1021/acscatal.9b04831
ACS Catal. XXXX, XXX, XXX−XXX

Deacetylase Inhibitors as Anticancer Agents. *Annu. Rev. Pharmacol. Toxicol.* **2005**, *45*, 495−528.
(92) Bell, R. P. The Theory of Reactions Involving Proton Transfers. *Proc. R. Soc. London, Ser. A* **1936**, *154*, 414−429.
(93) Evans, M.; Polanyi, M. Further Considerations on the Thermodynamics of Chemical Equilibria and Reaction Rates. *Trans. Faraday Soc.* **1936**, *32*, 1333−1360.
(94) Balandin, A. In *Advances in Catalysis*; Elsevier, 1969; Vol. *19*; pp 1−210.
(95) Li, H.; Qian, Z. M. Transferrin/Transferrin Receptor-Mediated Drug Delivery. *Med. Res. Rev.* **2002**, *22*, 225−250.
(96) Gupta, Y.; Jain, A.; Jain, S. K. Transferrin-Conjugated Solid Lipid Nanoparticles for Enhanced Delivery of Quinine Dihydrochloride to the Brain. *J. Pharm. Pharmacol.* **2007**, *59*, 935−940.
(97) Li, H.; Sadler, P. J.; Sun, H. Rationalization of the Strength of Metal Binding to Human Serum Transferrin. *Eur. J. Biochem.* **1996**, *242*, 387−393.
(98) Tinoco, A. D.; Valentine, A. M. Ti (IV) Binds to Human Serum Transferrin More Tightly Than Does Fe (III). *J. Am. Chem. Soc.* **2005**, *127*, 11218−11219.
(99) Tinoco, A. D.; Incarvito, C. D.; Valentine, A. M. Calorimetric, Spectroscopic, and Model Studies Provide Insight Into the Transport of Ti (IV) by Human Serum Transferrin. *J. Am. Chem. Soc.* **2007**, *129*, 3444−3454.
(100) Sun, H.; Li, H.; Sadler, P. J. Transferrin as a Metal Ion Mediator. *Chem. Rev.* **1999**, *99*, 2817−2842.
(101) Cini, M.; Bradshaw, T. D.; Woodward, S. Using Titanium Complexes to Defeat Cancer: the View From the Shoulders of Titans. *Chem. Soc. Rev.* **2017**, *46*, 1040−1051.
(102) Baker, H. M.; Nurizzo, D.; Mason, A. B.; Baker, E. N. Structures of Two Mutants that Probe the Role in Iron Release of the Dilysine Pair in the N-lobe of Human Transferrin. *Acta Crystallogr., Sect. D: Biol. Crystallogr.* **2007**, *63*, 408−414.
(103) Mujika, J. I.; Escribano, B.; Akhmatskaya, E.; Ugalde, J. M.; Lopez, X. Molecular Dynamics Simulations of Iron- and Aluminum-Loaded Serum Transferrin: Protonation of Tyr188 is Necessary to Prompt Metal Release. *Biochemistry* **2012**, *51*, 7017−27.
(104) Rinaldo, D.; Field, M. J. A Computational Study of the Open and Closed Forms of the N-lobe Human Serum Transferrin Apoprotein. *Biophys. J.* **2003**, *85*, 3485−3501.
(105) Dojindo Molecular Technologies, Inc. *I. Metal Chelates.* Accessed: 2019−09−18.
(106) Passer, E.; White, J.; Cheng, K. The Crystal Structure of $Mg_2EDTA \cdot 9H_2O$. *Inorg. Chim. Acta* **1977**, *24*, 13−23.
(107) Gaggioli, C. A.; Stoneburner, S. J.; Cramer, C. J.; Gagliardi, L. Beyond Density Functional Theory: the Multiconfigurational Approach to Model Heterogeneous Catalysis. *ACS Catal.* **2019**, *9*, 8481−8502.
(108) Gagliardi, L.; Truhlar, D. G.; Li Manni, G.; Carlson, R. K.; Hoyer, C. E.; Bao, J. L. Multiconfiguration Pair-Density Functional Theory: A New Way to Treat Strongly Correlated Systems. *Acc. Chem. Res.* **2017**, *50*, 66−73.

https://dx.doi.org/10.1021/acscatal.9b04831
ACS Catal. XXXX, XXX, XXX−XXX